
**AFRL-OSR-VA-TR-2014-0029**

# DYNAMICAL IMAGING USING SPATIAL NONLINEEARITY

**JASON FLEISCHER**

**PRINCETON UNIVERSITY**

**01/29/2014**
**Final Report**



**AIR FORCE RESEARCH LABORATORY**
**AF OFFICE OF SCIENTIFIC RESEARCH (AFOSR)/RSE**
**ARLINGTON, VIRGINIA 22203**
**AIR FORCE MATERIEL COMMAND**

# REPORT DOCUMENTATION PAGE

*Form Approved*
*OMB No. 0704-0188*



| **1. REPORT DATE** *(DD-MM-YYYY)* | **2. REPORT TYPE** | **3. DATES COVERED** *(From - To)* |
|---|---|---|
| 29-01-2014 | Final | 5/1/10-9/30/13 |

**4. TITLE AND SUBTITLE**

Dynamical imaging using spatial nonlinearity

**5a. CONTRACT NUMBER**

**5b. GRANT NUMBER**
FA9550-10-1-0108

**5c. PROGRAM ELEMENT NUMBER**
N/A

**6. AUTHOR(S)**
Fleischer, Jason W.

**5d. PROJECT NUMBER**
N/A

**5e. TASK NUMBER**
N/A

**5f. WORK UNIT NUMBER**
N/A

**7. PERFORMING ORGANIZATION NAME(S) AND ADDRESS(ES)**
Princeton University
P.O. Box 36
Princeton, NJ 08544-2020

**8. PERFORMING ORGANIZATION REPORT NUMBER**

**9. SPONSORING / MONITORING AGENCY NAME(S) AND ADDRESS(ES)**
Air Force Office of Scientific Research
875 North Randolph Road
Arlington, VA 22203

**10. SPONSOR/MONITOR'S ACRONYM(S)**

**11. SPONSOR/MONITOR'S REPORT NUMBER(S)**

**12. DISTRIBUTION / AVAILABILITY STATEMENT**
Approved for public release; distribution is unlimited

**13. SUPPLEMENTARY NOTES**

**14. ABSTRACT**

In this proposal, we used spatial nonlinearity as a degree of freedom for imaging. Mode mixing in nonlinear systems enables them to surpass many fundamental limits of conventional (linear) imaging, such as resolution and field of view, and can overcome many of its basic trade-offs, including resolution vs. contrast and signal vs. noise. The work expanded Abbe's 1873 theory of diffraction to include spatial nonlinearity, prompted new experimental methods of phase-space measurement, and facilitated the discovery of new optical dynamics. The results generalized the field of computational imaging, on both the physical and algorithmic layers, by introducing new spatial interactions between amplitude and phase. They also raised many new and outstanding issues that need to be addressed, such as the best types of nonlinearity to use, the uniqueness and robustness of solutions, the levels of improvement possible, and the information capacity of nonlinear systems. These issues lay the foundation for future work.

**15. SUBJECT TERMS**

Optics, nonlinearity, imaging

| **16. SECURITY CLASSIFICATION OF:** | | | **17. LIMITATION OF ABSTRACT** | **18. NUMBER OF PAGES** | **19a. NAME OF RESPONSIBLE PERSON** |
|---|---|---|---|---|---|
| **a. REPORT** | **b. ABSTRACT** | **c. THIS PAGE** | UU | 11 | Arje Nachman |
| U | U | U | | | **19b. TELEPHONE NUMBER** *(include area code)* 703-696-7797 |

# Dynamical imaging using spatial nonlinearity: *Final Report*

Jason Fleischer, Princeton University

All limitations commonly associated with imaging, such as resolution, field of view, and depth of field, arise from linear theory[1]. Nonlinear optics can break these limits by exploiting the presence and interaction of many photons at once. To date, nearly all nonlinear imaging techniques have relied on point processes, such as two-photon fluorescence[2] or harmonic effects[3], in which the temporal frequency is the relevant parameter. These methods ignore the spatial content of the object, typically require scanning to record a whole image, and remain restricted by linear propagation from the sample to the detector. Spatial nonlinearity can overcome these issues by mixing modes with high and low spatial frequencies.

In this proposal, we explored the dynamics of imaging using spatial nonlinearity. This included fundamental dynamics of spatial mode mixing, a nonlinear generalization of Abbe's 1873 theory of diffraction, phase retrieval using nonlinear diversity, and nonlinear signal-noise coupling. Below, we highlight each of these areas.

## Nonlinear Abbe Theory[4]

The limitations of linear imaging were formalized succinctly by Ernst Abbe in 1873 [1]. In his theory, an object is treated as an ensemble of Fourier modes, each of which acts individually as a diffraction grating. The observation of spatial features is then determined by the wavelength of the illumination light, which governs diffraction from the (virtual) grating, and the acceptance angle of system, given by the numerical aperture. Spatial modes can be detected only if the wavenumbers of the lowest diffraction orders lie within the spatial bandwidth of the system (Fig. 1a). Otherwise, they — and the corresponding features — are lost.

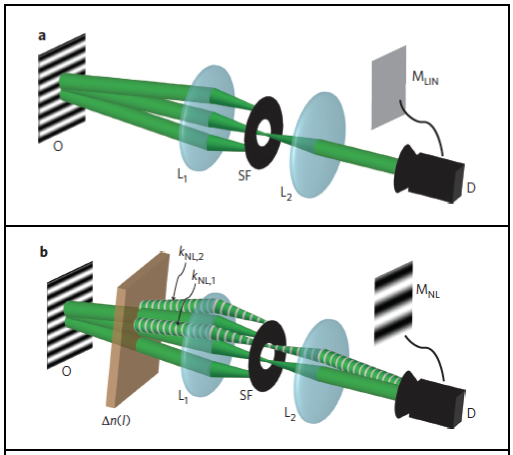


**Figure 1. Linear vs. nonlinear Abbe theory.** (a) In conventional, linear Abbe theory, object modes are treated as diffraction gratings. High-$k$ modes are blocked by the system's numerical aperture, so that the grating is not seen in the image plane. (b) In the presence of spatial nonlinearity, wave mixing generates daughter modes (striped), some of which can propagate to the detector plane. Interference is recorded and, with suitable knowledge of the medium response, computation can recover the original spatial features. O: object; $L_1$,$L_2$: lenses; SF: spatial filter; $M_{LIN}$, $M_{NL}$: Linear and nonlinear measurements, D: detector.

Interestingly, Abbe's theory also suggests means of imaging beyond the diffraction limit. Perhaps the most straightforward is the use of an additional diffraction grating[5] to shift high wavenumbers back into the field of view. Numerical processing can then reverse the shift to enable super-resolution of the object. Other computational methods also rely on *a priori* information, including "extra" knowledge of the field[6, 7], aperture location[8], transfer function[9, 10], and/or the illumination[11] or source[12-14] radiance. Nonlinear sources and objects have been used[2, 3], but to date the methods have considered only temporal frequency mixing. These are point processes that circumvent linear limits by generating shorter wavelengths, tighter focal spots, and less unwanted scattering. However, beam propagation from the sample to the detector is still linear, so that observations are still restricted by the numerical aperture of the system.

Abbe theory can be generalized in a straightforward manner to include spatial nonlinearity. The mechanism is best understood as a nonlinear version of structured illumination (SI). In SI, a pattern of light (typically periodic) is projected onto the object, and the resulting Moire fringes let high-$k$ modes originally outside of the observation window scatter into it. Numerical deconvolution is then used to

reconstruct the original signal modes[15]. However, removal of phase ambiguity requires lateral shifting of the grating, and 2D coverage in $k$-space requires rotation and multiple grating periods. In the nonlinear case (Fig. 1b), the object itself creates a spatially varying intensity pattern, $I(x)$, which in the nonlinear medium induces an index change $\Delta n = \Delta n(I)$. This index change is effectively a diffraction grating, which by construction is inherently phase-matched with the modes of the object.

Structured illumination can mimic the effects of nonlinearity by projecting a nonlinear (i.e. non-sinusoidal) pattern onto the object[16]. In this approach, the mixing of high and low wavenumbers occurs in a single plane. With bulk dynamics, there are three effects which work in concert: 1) generation of daughter waves from mode coupling, 2) changes in the parent waves, and 3) continuous evolution of (1) and (2) due to propagation. This latter property can both amplify the original changes as well as cascade them. While the particular wave mixing is object-dependent, its general features can expressed by a single nonlinear propagator[17, 18]. Once a given medium is characterized, numerical reconstruction (back-propagation) uses only measurements at the output and works for any object at the input[17, 19].

As an experimental proof of principle, we use as an input a grating-probe signal whose grating frequency is too high to pass through the filter (Fig. 2). Here, the probe to grating intensity ratio is 10:1. In the linear case, the grating modes are blocked, and only the uniform intensity of the plane-wave probe beam is measured. In the nonlinear case, the grating modes remain blocked, but a new mode, $k_{NL}$, is generated and detected. Interestingly, in this simple example, numerical back-propagation is not necessary to reconstruct the original modes. Because the system is known to be only weakly nonlinear, the dominant process is first-generation four-wave mixing. For a Kerr nonlinearity, the grating mode $k_g$ will couple with the probe $k_p$ to generate a mode at $k_{NL} = 2k_p - k_g$, which can be identified directly. By extension, this argument gives an upper bound to the resolution improvement in the weakly nonlinear case. Only modes that generate $k_{NL}$ within the observable spectral window, below the filter cutoff $k_{cut}$, can be measured, *i.e.* modes $k_{NL} < k_{cut}$ corresponding to $k_g < k_{cut} + 2k_P$. Since the probe beam $k_P$ also lies in the observable window, its maximum value is $k_{cut}$ as well. Therefore, the upper frequency bound of a grating mode is $3k_{cut}$, giving a resolution that is 3x that achievable in the linear case.

The improvement in resolution due to nonlinearity is theoretically unlimited[16], though some subtleties must be considered. On one hand, material response is separate from diffraction, so that nonlinear wave mixing works well beyond any paraxial approximation[20]. (Even adding high spatial harmonics numerically can be useful for imaging[21].) Physically, evanescent waves at interfaces can be controlled nonlinearly[22, 23], and structured illumination can be enhanced by saturation[16] and other nonlinear effects. On the other hand, the nonlinear modes generated by the response are still affected by diffraction; modes at the edges of the transmission window, in particular, compete with that part of the system transfer function. For a single image, the end result is a resonance effect (common to all nonlinear problems) in which the optimum represents a balance between the modes of the object, the information capacity of the system, and the nature of the medium response[24]. As in structured illumination, though, processing multiple images using successively wider windows of spatial frequency can compound the improvements. A detailed discussion of these issues can be found in the Supplement of Ref. [4].

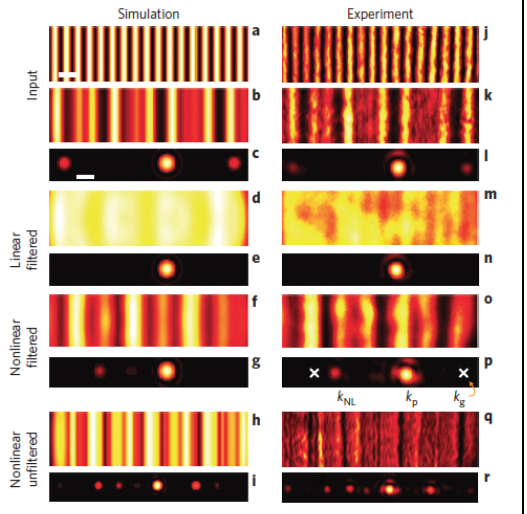


**Figure 2: Bandwidth extrapolation via spatial nonlinearity.** Left column, simulation; right column, experiment. a,b,c); j,k,l) Input signal. (a,j) input grating, (b,k) input grating + plane-wave probe beam, (c,l) $k$-space measurement, showing three main wavenumbers. d,e); m,n) Filtered linear signal (spatial filter SF closed), showing lost grating frequencies. f,g) ;o,p) Filtered nonlinear output: grating modes are still lost, but a nonlinearly generated daughter wave appears. Crosses mark calculated reconstruction of lost frequencies using only the two measured modes. h,i); q,r) Full object (SF open). Measured grating mode locations match calculation from nonlinear measurement. Scale bar: 85 μm for all real space images and $\pi/4.5$ μm$^{-1}$ for all k-space images except i,r), which are demagnified 1.5 times.

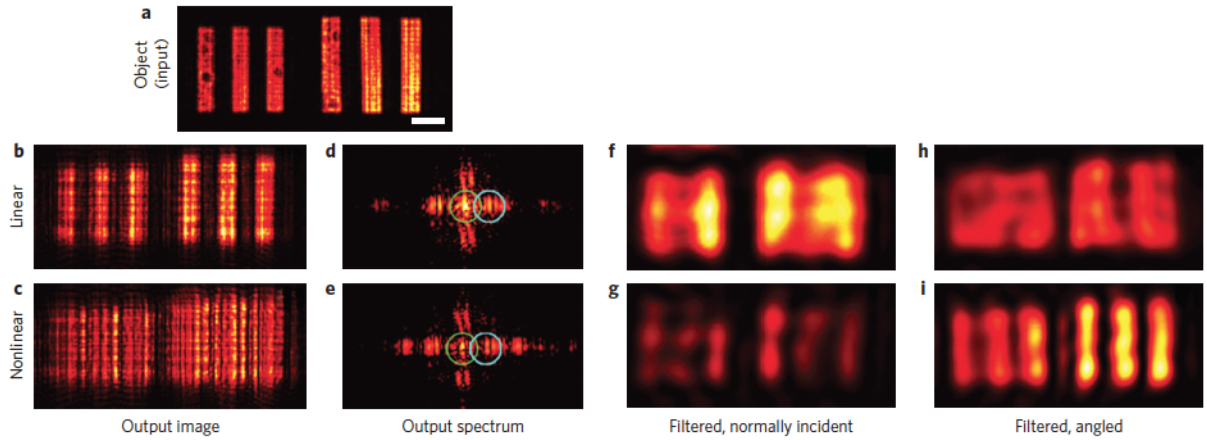


**Figure 3: Super-resolution via spatial nonlinearity.** a) Measured input and b,c) measured output intensities for (b) linear and (c) nonlinear propagation. d,e) Measured output spectrum for (d) linear and (e) nonlinear propagation. f,g) Linear and nonlinear intensity outputs with the spatial filter SF closed and the signal normally incident on the crystal. The SF allows the green circled regions in d,e) to pass. h,i) Linear and nonlinear intensity outputs with the spatial filter SF closed and the signal propagating at an angle. The SF allows the blue circled regions in d,e) to pass. Scale bar: 200 μm.

In the grating example, it was known *ab initio* that the number of high-$k$ modes outside the numerical aperture was limited. That is, there were no modes $k_>$ and $k_{>>}$ such that the beat frequency $k_{>>} - k_>$ appeared inside the observation window. For a more general object, this cannot be guaranteed. Even worse, there may be many such modes (potentially an infinite number, though their coupling is considerably more inefficient as the wavenumbers increase), as well as higher-order interactions. The former problem may be surmounted by changing the angle of the probe beam $k_p$; modes that mix with $k_p$ will shift along with it, while independent beat modes will not. In this regard, we note that a probe beam should be added to any object, both to rule out independent beating and to facilitate mode coupling in the first place[18]. For the problem of higher-order interactions, the intensity of the object or illumination can be varied, as the intensity of the output depends on the product of input amplitudes. However, recent experiments have shown that four-wave mixing is the dominant interaction during propagation[25], so that neglecting higher-order interactions is usually a valid approximation.

Besides resolution, there are other metrics of image quality that may take precedence, e.g. visibility of features for (automated) discrimination. An example is shown in Fig. 3. In the linear case, the output image is again diffraction-limited by the spatial filter, making the bars of the chart unrecognizable. In the nonlinear case, the bars are clear and distinct. The improvement can be quantified by the Rayleigh criterion, which corresponds to a minimum visibility $V = (I_{max} - I_{min})/ (I_{max} + I_{min}) = 0.15$ for detection of the bars (from maxima to central dip). For our experimental measurements, the *best* linear visibility is only *0.095*, while the *worst* visibility in the nonlinear regime is *0.32*. This is more than a threefold improvement, a result due not only to high-$k$ modes folding into the observation window but also to low-$k$ modes (esp. the $k$=0 DC term) scattering out of it. Spectral energy coupling can be observed directly by adjusting the spatial filter. When the filter is centered on the optic axis ($k = 0$), the nonlinear output power is significantly lower than the linear power. When the filter is shifted laterally by 5mrad, so that it is centered on the first-order diffraction lobe, the contrast and power are greatly increased. Interestingly, this improvement is object-dependent, implying that system performance can be optimized if the target is known. More generally, the results show that fundamental trade-offs in linear optics, such as resolution vs. contrast, need not apply in nonlinear imaging systems.

## Nonlinear phase retrieval[26]

One of the earliest and most important examples of computational imaging is phase retrieval. The most common example is the Gerchberg-Saxton algorithm[27], in which the phase is computed using intensity patterns measured at two different planes of propagation [typically the near-field (image) and far-field (Fourier) planes]. Other forms of parameter diversity, such as axial[28] and transverse[29, 30] displacement, wavelength[31], and polarization [7], have been used as well. These methods work because in beam propagation, dispersion and diffraction of spatial modes convert phase information into intensity.

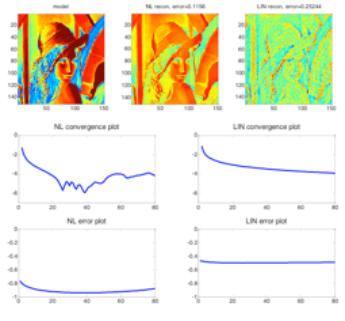


**Figure 4. Nonlinear phase matching.** Phase matching gives a convergence criterion for nonlinear phase retrieval, yielding faster convergence with lower error. Left: nonlinear; right: linear.

Nonlinear media provide an additional relationship between amplitude and phase through intensity-dependent changes to the refractive index. As a result, nonlinear systems provide a natural route toward contrast enhancement and increased sensitivity to phase[26, 32-38]. A comparison between linear and nonlinear phase retrieval is shown in Fig. 4. In each case, a uniform phase $\varphi = 0$ is used as input then iteratively approximated, using the two measured amplitudes as boundary conditions. Compared with linear phase retrieval, which is independent of amplitude and has a monotonic convergence behavior, nonlinear retrieval is much more complex. Object- and intensity-dependent phase-matching conditions give rise to resonant spikes in convergence. Typically, the largest spike sets a condition for stopping the iteration cycle, but more work needs to be done to prove this. Nevertheless, in all cases tested so far, nonlinearity yielded a faster convergence speed and a lower phase error than linear methods (both ~2x better).

## Nonlinear signal-noise coupling[39, 40]

Nonlinearity has a similarly dramatic effect on light that is partially spatially correlated. As with diffraction, spatial coherence can either compete or cooperate with nonlinearity, e.g. by inhibiting instabilities or generating new ones. In terms of information processing, there is a rich interplay between spatial nonlineairty, signal, and noise that is only just beginning to be explored[24]. For example, energy can transfer nonlinearly from noise to signal, resulting in a "stochastic resonance" that can boost the signal to detectability[41]. In contrast, mode mixing from nonlinearity can create an effective noise, reducing the information capacity of an optical system[24, 42].

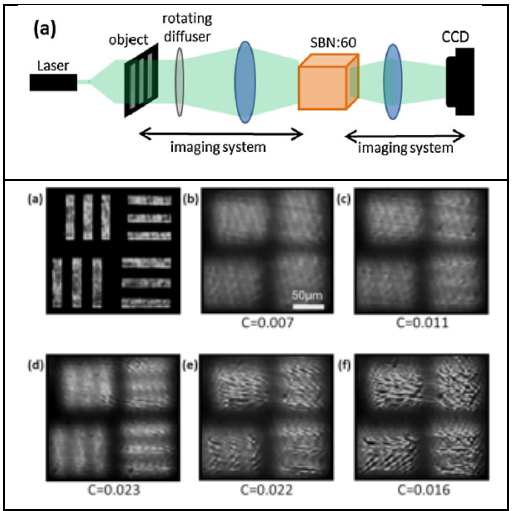


**Figure 5. Instability-driven recovery of diffused images.** (a) Experimental setup. (b-g) Experimental output with increasing nonlinearity. (b) Undiffused image of the resolution chart. (c) Output after linear propagation. (d) Nonlinear output for weak nonlinearity ($\delta n = 1.3\text{x}10^{-4}$). (e-g) Output for stronger nonlinearity, above the threshold for incoherent modulation instability ((e) $\delta n = 1.7\text{x}10^{-4}$, (f) $\delta n = 2.0\text{x}10^{-4}$, (g) $\delta n = 2.3\text{x}10^{-4}$). Numbers below the frames are the corresponding input-output correlation coefficients, $C = \left\langle I_{chart} \cdot I_{out}^{NL} \right\rangle$.

An example of nonlinear signal-noise coupling is shown in Fig. 5. Light from a 532nm laser is incident on a resolution chart followed by a holographic diffuser. A lens then images the resolution chart onto a photorefractive SBN:60 ($Sr_{0.6}Ba_{0.4}Nb_2O_6$) crystal. The role of the diffuser is to scatter light from the object, in a maner similar to clouds or tissue, so that the chart features are diffused and unrecognizable. In the experiment, the diffuser has a Gaussian angular spread of $0.5^{\circ}$ and is placed 15mm after the object, so that the correlation length ~ 100μm at the input face of the crystal. To give a uniform, rather than speckled, input pattern, the diffuser is rotated at a rate (~200Hz) that is

much faster than the response time of the crystal (~1s). Figure 5b shows the input pattern without the diffuser, while Fig. 5c shows the time-averaged pattern when the diffuser is rotated. For SBN, the nonlinear index change is $\Delta n = \kappa E_{app}\langle I\rangle/(1+\langle I\rangle)$, where $\langle I\rangle$ is an intensity perturbation above a spatially homogeneous background intensity $\langle I_0\rangle$, $E_{\text{app}}$ is an electric field applied across the crystalline c-axis, and $\kappa = n_o r_{33}(1+\langle I_0\rangle)$ is a constant depending on the base index of refraction $n_o$, the electro-optic coefficient $r_{33}$, and $\langle I_0\rangle$ [43]. Here, the brackets $\langle\ \ \rangle$ denote a time average., where the integration time $\tau$ is longer than the time scale of fast phase fluctuations $\tau_\varphi$ but shorter than the slow response time $\tau_r$ the photorefractive crystal (*i.e.* $\tau_\varphi < \tau < \tau_r$). For the experiments, the illumination intensity is kept a constant 10μW and a self-focusing nonlinearity is created and controlled by varying an applied voltage bias across the crystal. Light exiting the nonlinear crystal is then imaged onto a CCD camera.

Scattered images like the one in Fig. 5c are partially coherent and can be characterized as a statistical ensemble of spatial modes. For the geometry here, the field passing through the chart is effectively multiplied by many realizations of the diffuser transmission function (a random pure-phase plate), so that the initial image cannot be reconstructed by simple linear averaging[44]. On the other hand, the modes of the product beam are not entirely random; there are correlations due to the original image. In a nonlinear medium, these modes can interact dynamically as they propagate. For simple (e.g. homogeneous) beams, possible results include suppressed or enhanced diffraction[45], instabilities[46-48], and spatial optical turbulence[49]. For beams with initial correlations, the dynamics are preferentially biased. In particular, signal modes can reinforce each other and extract energy from the diffuse background, growing as they propagate. For example, a Kerr-type nonlinearity $\Delta n = \gamma\left\langle \psi(x)\psi^*(x)\right\rangle$, where $\gamma$ is the nonlinear coefficient and $\psi$(x) is the wave-field, gives a convolution of modes in Fourier space, $\Delta n = \gamma\int dk'\left\langle \hat{\psi}(k')\hat{\psi}^*(k-k')\right\rangle$, so that any correlations in the wavefunction $\psi$ will influence the subsequent nonlinear response. If an instability is seeded, then exponential growth of the signal is possible.

An experimental demonstration of this dynamics is given in Fig. 5, which shows the output face of the crystal as the nonlinear coupling strength is increased. As in the simulations, there is no visible change in the output pattern until a threshold is reached (Figs. 5c,d), after which the quality of the image degrades. A measure of the image quality can be obtained by computing the cross- correlation $C = \int\left\langle I_{chart}\cdot I_{out}^{NL}\right\rangle dx$ between an ideal input chart ($I_{\text{chart}}$ = 1 at the bars and zero elsewhere) and the measured output intensity. These values are shown beneath the frames in Fig. 5.

**Phase-space optics[50]**

Phase-space representations simultaneously store spatial and spatial frequency information, in a manner analogous to the position-momentum representation in mechanics. Indeed, under the common assumption that the coherence time of the wave-field is much shorter than the response time of the camera (typical of most non-laser sources), a Hamiltonian or eikonal description of wave evolution is suitable[51]. Accordingly, any (nonlinear) dynamics that can benefit from a Hamiltonian description would best be treated by a phase-space representation.

There are many choices of functions that represent phase space. Perhaps the most popular is the time-averaged Wigner distribution function (WDF), defined as

$$f(r,k) = \int\left\langle \psi^*(r+\xi/2)\psi(f-\xi/2)e^{ik\xi}\right\rangle d\xi$$

where r = (x,y) and k = ($k_x$, $k_y$) are the 2D spatial and spatial frequency vectors, respectively[52]. This form is essentially a Fourier transform of the two-point correlation function, so retains local information about intensity and momentum (Poynting vector). In the coherent limit, the WDF is highly redundant, since coherent light at a single position is associated with only a single direction (phase). Only a 2D

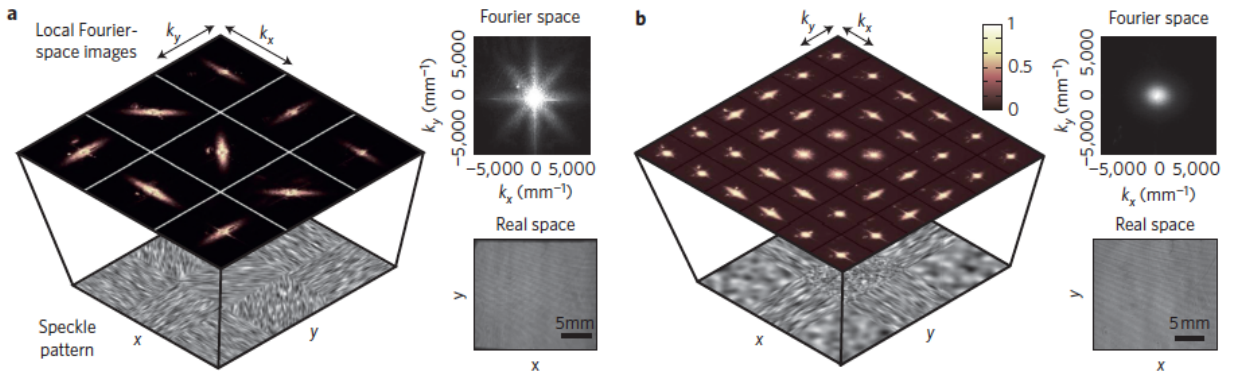


**Figure 6. Experimental creation and measurement of beams with arbitrary spatial coherence.** An input spatial light modulator (SLM) creates a time-multiplexed speckle beam and a measurement SLM uses a scanning aperture to record a windowed Fourier transform of the time-averaged pattern. Subplots show the local Fourier power spectra (spatial frequency distributions) as a function of position. Top: local power spectrum at different points in (x,y). Bottom: intensity image of one representation of a random speckle pattern at the input (diffuser) SLM. For comparison, the standard measurements of real-space and Fourier-space images, taken without using the aperture on the output SLM, are shown to the right of each figure. a) Elliptical speckles, which rotate across the beam. b) Gaussian speckles, with varying widths across the beam.

description is necessary, with two projections of the WDF being sufficient to recover the entire wave-field uniquely[53]. In contrast, phase-space distributions of partially coherent beams are usually not redundant, as coherence information fills up more of the 4D phase space[54].

Until our work, nearly all measurements in linear optics, and all those in nonlinear optics, recorded only the marginals of the WDF, i.e. the intensity and power spectrum projections $I(r) = \int f(r,k)\,dk$ and $I(k) = \int f(r,k)\,dr$

This means that coherence properties that change as a function of transverse position, as well as more complex phase-space structures, have eluded observation. Correspondingly, there has been limited motivation to generate arbitrary, spatially varying patterns of coherence, especially for two-dimensional beams. We remedied both problems in this proposal, using spatial light modulators for both coherence synthesis and phase-space measurement.

Examples of 4D coherence control and measurement are shown in Fig. 6. Figure 6 shows two different beams that have homogeneous real space intensities but varying coherence properties across both axes of **r**. The first example (Fig. 6a) uses elliptically shaped speckles, whose orientation is rotated in different parts of the field of view. For clarity, we show only one realization of an ensemble of 50 speckle patterns having the same spatial statistics but different random implementations of speckle; the integrated real-space intensity contains no information about the coherence of the beam, while the Fourier-domain intensity is a projection over all **r** and cannot reveal the spatial variations of coherence properties. In contrast, local *k*-space images (taken by the Fourier CCD with the SLM aperture in different locations) do give information about the local coherence properties. A similar example is given in Fig 6b, which shows a beam designed to have anisotropic Gaussian statistics with an ellipticity that varies according to position. Two-dimensional beams with such local variations of coherence properties had not, to our knowledge, been created and measured previously.

## Conclusions

In this proposal, we used spatial nonlinearity as a degree of freedom for imaging. The mode mixing which results enables the breaking of many fundamental limits of conventional (linear) imaging, including resolution and field of view, and can overcome many of the basic trade-offs, including resolution vs. contrast and signal vs. noise. In terms of optical science, the work expanded Abbe's 1873 theory of

diffraction to include spatial nonlinearity, prompted the development of new experimental methods of phase-space measurement, and facilitated the discovery of new nonlinear dynamics. In terms of imaging, the results generalized the field of computational imaging, on both the device and algorithmic levels. They also introduced many new and outstanding issues that need to be addressed, such as the best types of nonlinearity to use, the uniqueness and robustness of solutions, the levels of improvement possible, and the information capacity of nonlinear systems. These will be explored in future work.

**Appendix: Publications resulting from the grant**

1. "Nonlinear Abbe theory"
   Christopher Barsi and Jason W. Fleischer, Nature Photonics **7**, 639 (2013).

2. "Quantitative amplification of weak images by nonlinear propagation"
   Laura Waller, Dmitry V. Dylov, and Jason W. Fleischer, Optics Letters **38**, 82 (2013).

3. "Phase retrieval using nonlinear diversity"
   Chien-Hung Lu, Christopher Barsi, Matthew O. Williams, Nathan Kutz, and Jason W. Fleischer, Applied Optics **52**, D92 (2013).

4. "Enhancing layered 3D imaging with a lens"
   Stefan Muenzel and Jason W. Fleischer, Applied Optics **52**, D97 (2013).

5. "Observation of the kinetic condensation of classical waves"
   Can Sun, Shu Jia, Christopher Barsi, Sergio Rica, Antonio Picozzi, and Jason W. Fleischer, Nature Physics **8**, 470 (2012).

6. "Phase-space measurement and coherence synthesis of optical beams"
   Laura Waller, Guohai Situ, and Jason W. Fleischer, Nature Photonics **6**, 474 (2012).

7. "Wrinkles and deep folds as photonic structures in photovoltaics"
   Jong Bok Kim, Pilnam Kim, Nicolas C. Pégard, Soong Ju Oh, Cherie R. Kagan, Jason W. Fleischer, Howard A. Stone, and Yueh-Lin Loo, Nature Photonics **6**, 327 (2012).

8. "Spectral dynamics of spatially incoherent modulation instability"
   Can Sun, Laura Waller, Dmitry V. Dylov, and Jason W. Fleischer, Physical Review Letters **108**, 263902 (2012).

9. "Nonlinear restoration of diffused images via seeded instability" (Invited)
   Dmitry V. Dylov, Laura Waller, and Jason W. Fleischer, IEEE Journal of Quantum Electronics **18**, 916 (2012).

10. "Instability-driven recovery of diffused images"
    Dmitry V. Dylov, Laura Waller, and Jason W. Fleischer, Optics Letters **36**, 3711 (2011).

11. "Optimizing holographic data storage using fractional Fourier transforms"
    Nicolas C. Pégard and Jason W. Fleischer, Optics Letters **36**, 2551 (2011).

12. "Diffraction from an edge in a self-focusing medium"
    Wenjie Wan, Dmitry V. Dylov, Chris Barsi, and Jason W. Fleischer, Optics Letters **35**, 2819 (2010).

## References


[1] E. Abbe, Beiträge zur Theorie des Mikroskops und der micrkoskopischen Wahrnehmung, Arch. Mikrosk. Anat., 9 (1873) 413–468.

[2] W. Denk, J.H. Strickler, W.W. Webb, 2-Photon Laser Scanning Fluorescence Microscopy, Science, 248 (1990) 73-76.

[3] P.J. Campagnola, H.A. Clark, W.A. Mohler, A. Lewis, L.M. Loew, Second-harmonic imaging microscopy of living cells, J Biomed Opt, 6 (2001) 277-286.

[4] C. Barsi, J.W. Fleischer, Nonlinear Abbe theory, Nat Photonics, 7 (2013) 639-643.

[5] R. Heintzmann, C. Cremer, Lateral modulated excitation microscopy: Improvement of resolution by using a diffraction grating, Proceedings of the SPIE, 3568 (1999) 185-196.

[6] T. Di Francia, Resolving power and inforamtion, Journal of the Optical Society of America, 45 (1955) 497-501.

[7] I.F. Gorodnitsky, B.D. Rao, Sparse signal reconstruction from limited data using FOCUSS: A re-weighted minimum norm algorithm, Ieee T Signal Proces, 45 (1997) 600-616.

[8] E.A. Ash, G. Nicholls, Super-Resolution Aperture Scanning Microscope, Nature, 237 (1972) 510-&.

[9] W.A. Carrington, R.M. Lynch, E.D.W. Moore, G. Isenberg, K.E. Fogarty, F.S. Fredric, Superresolution 3-Dimensional Images of Fluorescence in Cells with Minimal Light Exposure, Science, 268 (1995) 1483-1487.

[10] S.R.P. Pavani, M.A. Thompson, J.S. Biteen, S.J. Lord, N. Liu, R.J. Twieg, R. Piestun, W.E. Moerner, Three-dimensional, single-molecule fluorescence imaging beyond the diffraction limit by using a double-helix point spread function, Proceedings of the National Academy of Sciences of the United States of America, 106 (2009) 2995-2999.

[11] M.G.L. Gustafsson, Surpassing the lateral resolution limit by a factor of two using structured illumination microscopy, Journal of Microscopy-Oxford, 198 (2000) 82-87.

[12] T.A. Klar, S.W. Hell, Subdiffraction resolution in far-field fluorescence microscopy, Optics Letters, 24 (1999) 954-956.

[13] M.J. Rust, M. Bates, X.W. Zhuang, Sub-diffraction-limit imaging by stochastic optical reconstruction microscopy (STORM), Nat Methods, 3 (2006) 793-795.

[14] E. Betzig, G.H. Patterson, R. Sougrat, O.W. Lindwasser, S. Olenych, J.S. Bonifacino, M.W. Davidson, J. Lippincott-Schwartz, H.F. Hess, Imaging intracellular fluorescent proteins at nanometer resolution, Science, 313 (2006) 1642-1645.

[15] W. Lukosz, M. Marchand, Optischen Abbildung Unter Überschreitung der Beugungsbedingten Auflösungsgrenze, Optica Applicata, 10 (1963) 241-245.

[16] M.G.L. Gustafsson, Nonlinear structured-illumination microscopy: Wide-field fluorescence imaging with theoretically unlimited resolution, Proceedings of the National Academy of Sciences of the United States of America, 102 (2005) 13081-13086.

[17] C. Barsi, W. Wan, J.W. Fleischer, Imaging through nonlinear media using digital holography, Nat Photonics, 3 (2009) 211-215.

[18] W. Wan, S. Jia, J.W. Fleischer, Dispersive superfluid-like shock waves in nonlinear optics, Nature Physics, 3 (2007) 46-51.

[19] M. Tsang, D. Psaltis, F.G. Omenetto, Reverse propagation of femtosecond pulses in optical fibers, Optics Letters, 28 (2003) 1873-1875.

[20] M.D. Feit, J.A. Fleck, Beam Nonparaxiality, Filament Formation, and Beam Breakup in the Self-Focusing of Optical Beams, Journal of the Optical Society of America B-Optical Physics, 5 (1988) 633-640.

[21] H. Greenspan, C. Anderson, S. Akber, Image enhancement by nonlinear extrapolation in frequency space, Ieee Transactions on Image Processing, 9 (2000) 1035-1048.

[22] J. Renger, R. Quidant, N. van Hulst, L. Novotny, Surface-Enhanced Nonlinear Four-Wave Mixing (vol 104, art no 046803, 2010), Physical Review Letters, 104 (2010).

[23] O. Emile, T. Galstyan, A. Lefloch, F. Bretenaker, Measurement of the Nonlinear Goos-Hanchen Effect for Gaussian Optical Beams, Physical Review Letters, 75 (1995) 1511-1513.

[24] D.V. Dylov, J.W. Fleischer, Nonlinear self-filtering of noisy images via dynamical stochastic resonance, Nat Photonics, 4 (2010) 323-327.

[25] C. Sun, S. Jia, C. Barsi, S. Rica, A. Picozzi, J.W. Fleischer, Observation of the kinetic condensation of classical waves, Nature Physics, 8 (2012) 471-475.

[26] C.H. Lu, C. Barsi, M.O. Williams, J.N. Kutz, J.W. Fleischer, Phase retrieval using nonlinear diversity, Applied Optics, 52 (2013) D92-D96.

[27] R.W. Gerchberg, A practical algorithm for the determination of phase from image and diffraction plane pictures, Optik, (1972).

[28] R.A. GONSALVES, Phase Retrieval and Diversity in Adaptive Optics, Optical Engineering, 21 (1982) 829-832.

[29] H. Faulkner, J. Rodenburg, Movable Aperture Lensless Transmission Microscopy: A Novel Phase Retrieval Algorithm, Physical Review Letters, 93 (2004) 023903.

[30] F. Zhang, G. Pedrini, W. Osten, Phase retrieval of arbitrary complex-valued fields through aperture-plane modulation, Physical Review A, 75 (2007) 043805.

[31] H.R. Ingleby, D.R. McGaughey, Parallel multiframe blind deconvolution using wavelength diversity, in: P.J. Bones, M.A. Fiddy, R.P. Millane (Eds.) Optical Science and Technology, the SPIE 49th Annual Meeting, SPIE, 2004, pp. 58-64.

[32] P.J. Bardroff, U. Leonhardt, W.P. Schleich, Adaptive phase retrieval of nonlinear waves, Optics communications, 147 (1998) 121-125.

[33] D. Paganin, K.A. Nugent, Phase measurement of waves that obey nonlinear equations, Optics letters, 27 (2002) 622-624.

[34] Y.-R. Tan, D. Paganin, R. Yu, M. Morgan, Wave-function reconstruction of complex fields obeying nonlinear parabolic equations, Physical Review E, 68 (2003) 066602.

[35] M. Puida, F. Ivanauskas, Light beam phase retrieval in nonlinear media: a computer simulation, Liet Matem Rink, (2005).

[36] A. Martin, L. Allen, Measuring the phase of a Bose-Einstein condensate, Physical Review A, 76 (2007) 053606.

[37] S.-W. Bahk, J.D. Zuegel, J.R. Fienup, C.C. Widmayer, J. Heebner, Spot-shadowing optimization to mitigate damage growth in a high-energy-laser amplifier chain, Applied Optics, 47 (2008) 6586-6593.

[38] V.Y. IVANOV, V.P. SIVOKON, M.A. VORONTSOV, Phase Retrieval From a Set of Intensity Measurements - Theory and Experiment, Journal of the Optical Society of America a-Optics Image Science and Vision, 9 (1992) 1515-1524.

[39] D.V. Dylov, L. Waller, J.W. Fleischer, Instability-driven recovery of diffused images, Optics Letters, 36 (2011) 3711-3713.

[40] D.V. Dylov, L. Waller, J.W. Fleischer, Nonlinear restoration of diffused images via seeded instability, IEEE Journal of Quantum Electronics, 18 (2012) 916-925.

[41] L. Gammaitoni, P. Hanggi, P. Jung, F. Marchesoni, Stochastic resonance, Reviews of Modern Physics, 70 (1998) 223-287.

[42] P.P. Mitra, J.B. Stark, Nonlinear limits to the information capacity of optical fibre communications, Nature, 411 (2001) 1027-1030.

[43] D.N. Christodoulides, T.H. Coskun, M. Mitchell, M. Segev, Theory of incoherent self-focusing in biased photorefractive media, Physical Review Letters, 78 (1997) 646-649.

[44] K. Kondo, Y. Ichioka, T. Suzuki, Image-Restoration by Wiener Filtering in Presence of Signal-Dependent Noise, Applied Optics, 16 (1977) 2554-2558.

[45] C. Sun, D.V. Dylov, J.W. Fleischer, Nonlinear focusing and defocusing of partially-coherent spatial beams, Optics Letters, 34 (2009) 3003-3005.

[46] M. Soljacic, M. Segev, T. Coskun, D.N. Christodoulides, A. Vishwanath, Modulation instability of incoherent beams in noninstantaneous nonlinear media, Physical Review Letters, 84 (2000) 467-470.

[47] D. Kip, M. Soljacic, M. Segev, E. Eugenieva, D.N. Christodoulides, Modulation instability and pattern formation in spatially incoherent light beams, Science, 290 (2000) 495-498.

[48] D.V. Dylov, J.W. Fleischer, Observation of all-optical bump-on-tail instability, Physical Review Letters, 100 (2008) 103903.

[49] D.V. Dylov, J.W. Fleischer, Multiple-stream instabilities and soliton turbulence in photonic plasma, Physical Review A, 78 (2008) 061804.

[50] L. Waller, G. Situ, J.W. Fleischer, Phase-space measurement and coherence synthesis of optical beams, Nat Photonics, 6 (2012) 474-479.

[51] B. Hall, M. Lisak, D. Anderson, R. Fedele, V.E. Semenov, Statistical theory for incoherent light propagation in nonlinear media, Physical Review E, 65 (2002) 035602.

[52] M.J. Bastiaans, Application of the Wigner Distribution Function to Partially Coherent-Light, Journal of the Optical Society of America a-Optics Image Science and Vision, 3 (1986) 1227-1238.

[53] M.E. Testorf, B.M. Hennelly, J. Ojeda-Castañeda, Phase-space optics : fundamentals and applications, McGraw-Hill, New York, 2010.

[54] K.H. Brenner, J. Ojedacastaneda, Ambiguity Function and Wigner Distribution Function Applied to Partially Coherent Imagery, Opt Acta, 31 (1984) 213-223.